PRAMANA
— journal of
physics

Vol. 62, No. 4
April 2004
pp. 957–965

Cluster radioactivity in xenon isotopes

K P SANTHOSH[1] and ANTONY JOSEPH[2]
[1]Department of Physics, Payyanur College, Payyanur 670 327, India
[2]Department of Physics, Calicut University, Calicut 673 635, India
E-mail: ajvar@rediffmail.com

MS received 1 March 2002; revised 15 September 2003; accepted 30 October 2003

Abstract. Half-life time and branching ratio for cluster decay from various xenon isotopes are studied taking Coulomb and proximity potentials as interacting barrier. Inclusion of proximity potential reduces the height of potential barrier, which closely agrees with the experiments. It is found that ^{4}He, ^{8}Be, ^{12}C and ^{16}O emissions are well within the present upper limit for measurements ($T_{1/2} < 10^{30}$ s). Our predicted half-life time values lie close to those values reported by Gupta and collaborators based on preformed cluster model (PCM) and also with those values reported by Poenaru *et al* based on ASAFM. The calculated half-life time shows that ^{8}Be from ^{108}Xe and ^{110}Xe are most favourable for emission ($T_{1/2} \approx 10^{8}$ s). Lowest $T_{1/2}$ value for ^{8}Be emission from ^{108}Xe stress the role of doubly magic ^{100}Sn daughter in cluster decay process. The logarithm of half-life time calculated for ^{4}He emission from ^{110}Xe is -0.39 s which is in good agreement with experimental value which is -0.40 s. Geiger–Nuttall plots for all clusters are studied and are found to be linear. Nuclear structure effect and shell effect are evident from the observed variation in slope and intercept of Geiger–Nuttall plots. It is found that neutron excess in the parent will slow down the cluster decay process.

Keywords. Cluster decay; exotic decay.

PACS Nos 23.70.+j; 23.60.+e

1. Introduction

The radioactive decay of nuclei emitting particle heavier than α-particle termed as exotic decay or cluster radioactivity was first predicted by Sandulescu *et al* [1] in 1980 on the basis of quantum mechanical fragmentation theory (QMFT) [2]. This rare, cold (neutron-less) process is intermediate between α-decay and sponteneous fission. The rare nature of this process is due to the fact that cluster emission is masked by several α-emissions. Experimentally, Rose and Jones [3] first observed such decays in 1984 in the radioactive decay of ^{223}Ra by the emission of ^{14}C.

The instabilities against exotic cluster decay of 'stable' nuclei in the region $Z =$ 50–82 was first pointed out by Gupta *et al* [4] in 1993. Within analytical superasymmetric fission model (ASAFM) Poenaru *et al* [5], within preformed cluster

model (PCM) Kumar *et al* [6] and within cubic plus Yukawa plus exponential potential model (CYEM) Shanmugam *et al* [7] calculated half-life time for the decay of proton-rich parents with $Z = 54$–64 and $N = 54$–72 emitting clusters ranging from ^{8}Be to ^{28}Si. This region is very interesting because daughter nuclei formed in such decays are doubly magic or near doubly magic ^{100}Sn nuclei and estimated half-life time for such decays are favourable for measurement. Moreover, these nuclei which are far from β stability line can be produced in a reaction induced by radioactive beams.

Cluster decay from this region (trans-tin region) was first experimentally done by Oganessian *et al* [8] at Dubna (Russia) and later by Guglielmetti *et al* [9] at GSI (Germany). In both experiments Ba isotope was produced using on-line mass separator by ^{58}Ni(^{58}Ni, $2n$) reaction and carbon clusters were searched for by means of solid state nuclear track detectors (SSNTD), of the polycarbonate and glass type in the Dubna and GSI experiments respectively.

Taking Coulomb and proximity potentials as interacting barrier we studied the cluster emission from various Ba isotopes [10,11] and Ce isotopes [12] using different mass tables. We found that ^{114}Ba was the best parent for ^{12}C emission and ^{116}Ce was the best parent for ^{16}O emission. In the present paper we extended our studies to various Xe isotopes emitting clusters ranging from ^{4}He to ^{28}Si. In the present study we have considered only α-nucleus clusters ($A_2 = 4n$, $Z_2 = N_2$) because it is now well-established by Kumar and collaborators [6] that α-nucleus clusters are most favourable for emission from Xe–Gd parents, which are evident from the deep minima in fragmentation potential for these clusters. The details of the model are given in §2 and results, discussion and conclusion are given in §3.

2. The model

The interacting barrier for a parent exhibiting exotic decay is given by

$$V = \frac{Z_1 Z_2 e^2}{r} + V_{\rm p}(z) + \frac{\hbar^2 \ell(\ell+1)}{2\mu r^2}, \quad \text{for } z > 0. \tag{1}$$

Here Z_1 and Z_2 are the atomic numbers of daughter and emitted cluster, r is the distance between the fragment centers, z is the distance between the near surface of the fragments and ℓ is the angular momentum. The mass parameter is replaced by reduced mass $\mu = mA_1A_2/A$ where m is the nucleon mass and A, A_1, A_2 represent mass numbers of the parent, daughter and emitted cluster respectively. $V_{\rm p}$ is the proximity potential given by Blocki *et al* [13].

$$V_{\rm p}(z) = 4\pi\gamma b \frac{C_1 C_2}{C_1 + C_2} \phi\left(\frac{z}{b}\right) \tag{2}$$

with nuclear surface tension coefficient

$$\gamma = 0.9517[1 - 1.7826(N-Z)^2/A^2] \text{ MeV fm}^{-2}. \tag{3}$$

Here N and Z represent neutron and proton numbers respectively of the parent. ϕ, the universal proximity potential is given as [14]

$$\phi(\varepsilon) = -4.41\mathrm{e}^{-\varepsilon/0.7176} \quad \text{for } \varepsilon \geq 1.9475, \tag{4}$$

$$\phi(\varepsilon) = -1.7817 + 0.9270\varepsilon + 0.01696\varepsilon^2 - 0.05148\varepsilon^3 \quad \text{for } 0 \leq \varepsilon \leq 1.9475, \tag{5}$$

with $\varepsilon = z/b$, where the width (diffuseness) of nuclear surface $b \approx 1$ and Siissmann central radii C_i related to sharp radii R_i is $C_i = R_i - (b^2/R_i)$. For R_i we use semi-empirical formula in terms of mass number A_i as [13]

$$R_i = 1.28A_i^{1/3} - 0.76 + 0.8A_i^{-1/3}. \tag{6}$$

The barrier penetrability P is given as

$$P = \exp\left\{-\frac{2}{\hbar}\int_{\varepsilon_i}^{\varepsilon_f}[2\mu(V-Q)]^{1/2}\mathrm{d}z\right\}. \tag{7}$$

The inner and outer turning points ε_i and ε_f are defined as $V(\varepsilon_i) = V(\varepsilon_f) = Q$, where Q is the energy released. The half-life time is given by

$$T_{1/2} = \ln 2/\lambda = \ln 2/\nu P. \tag{8}$$

Here λ is the decay constant and assault frequency, $\nu = 2E_\mathrm{v}/h$. The empirical zero point vibration energy E_v is given as [15]

$$E_\mathrm{v} = Q\{0.056 + 0.039\exp[(4-A_2)/2.5]\} \quad \text{for } A_2 \geq 4. \tag{9}$$

3. Results, discussion and conclusion

For touching and for separated configurations we took interacting barrier as the sum of Coulomb and proximity potentials. For overlap region we use simple power law interpolation as done by Shi and Swiatecki [16]. In the present model, assault frequency is calculated for each parent-cluster combination which is associated with zero point vibration energy but Shi and Swiatecki empirically got unrealistic values 10^{22} for even A parent and 10^{20} for odd A parent. Proximity potential was first used by Shi and Swiatecki in an empirical manner and has been quite extensively used by Malik and Gupta [17] in preformed cluster model (PCM) which is based on the 'pocket formula' of Blocki *et al* [13] which is given as

$$\phi(\varepsilon) = -(1/2)(\varepsilon - 2.54)^2 - 0.0852(\varepsilon - 2.54)^3 \quad \text{for } \varepsilon \leq 1.2511, \tag{10}$$

$$\phi(\varepsilon) = -3.437\exp(-\varepsilon/0.75) \quad \text{for } \varepsilon \geq 1.2511. \tag{11}$$

In the present model we use another formulation of proximity potential [14] given in eqs (4) and (5). Introduction of proximity potential reduces the height of potential barrier, which closely agrees with the experiments. Table 1 gives the comparison

Table 1. Comparison of interacting barrier height calculated by the present model with that by other models and with experimental values.

Parent nuclei	Emitted cluster	Daughter nuclei	Q value (MeV)	Barrier height (MeV)			
				LDM	CYEM	Present	Expt.
^{221}Fr	^{14}C	^{207}Tl	31.28	37.3448	26.6349	26.7625	28.448
^{221}Ra		^{207}Pb	32.39	37.0821	26.2740	26.3948	28.270
^{222}Ra		^{208}Pb	33.05	36.3428	25.5570	25.6768	27.290
^{223}Ra		^{209}Pb	31.85	37.4639	26.7025	26.8193	28.490
^{224}Ra		^{210}Pb	30.53	38.7056	27.9625	28.0823	29.810
^{225}Ac		^{211}Bi	30.48	39.5209	28.7198	28.8144	30.473
^{226}Ra		^{212}Pb	28.21	40.8700	30.1728	30.2898	32.130
^{231}Pa	^{24}Ne	^{207}Tl	60.42	47.7894	33.6222	33.1935	32.388
^{232}U		^{208}Pb	62.31	47.1171	32.8608	32.4000	31.519
^{233}U		^{209}Pb	60.50	48.8095	34.5784	34.1189	33.329

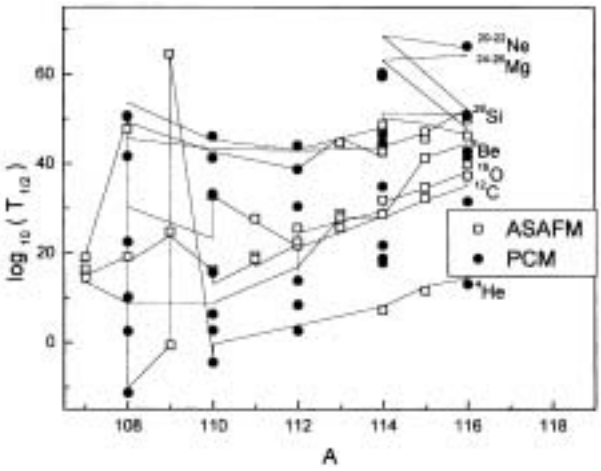

Figure 1. Logarithm of calculated half-life time vs. mass of Xe parents for various cluster emissions.

of the barrier height calculated by us taking proximity potential (present) with those obtained by liquid drop model (LDM) [18], by cubic plus Yukawa plus exponential potential model (CYEM) [19] and also with experimental values obtained by the relation [20]

$$V(r) = 10.107 + 0.1021 Z_1 Z_2 - Q. \tag{12}$$

It is clear that LDM overestimates the barrier by about 10 MeV but as in the case of CYEM, the present model is able to reproduce experimental values, which are uncertain by about 2 MeV [21].

Tables 2 and 3 give calculated half-life time and other characteristics for ^{4}He and ^{24}Mg emissions from various Xe isotopes and their comparison with PCM and ASAFM. Figure 1 gives $\log_{10}(T_{1/2})$ for ^{4}He, ^{8}Be, ^{12}C, ^{16}O, ^{20}Ne, ^{22}Ne, ^{24}Mg, ^{26}Mg

Table 2. Logarithm of predicted half-life time and other characteristics of ^{4}He emission from various Xe isotopes. Q values are taken from [5,6,22].

Parent nuclei	Emitted cluster	Daughter nuclei	Q value (MeV)	Penetrability P	Decay constant	$\log_{10}(T_{1/2})$			
						Present	ASAFM	PCM	Expt.
^{107}Xe	^{4}He	^{103}Te	1.89	2.60812E-40	2.26469E-20	19.49	19.0		
^{108}Xe		^{104}Te	0.88	5.21939E-70	2.11019E-50	49.52	47.7		
			6.49	3.41605E-11	1.01856E+10	−10.2		−11.26	
^{109}Xe		^{105}Te	3.99	1.47879E-20	2.71079	−0.59	−0.7		
			0.65	2.82177E-85	8.42663E-66	64.92	64.6		
^{110}Xe		^{106}Te	4.49	4.57764E-18	9.44293E+03	−3.13		−4.48	
			3.88	1.02254E-20	1.82278	−0.39			−0.40
^{112}Xe		^{108}Te	3.31	8.10013E-25	1.23179E-04	3.75		2.54	
^{114}Xe		^{110}Te	2.80	5.40006E-29	6.94664E-09	7.99	7.10		
^{115}Xe		^{111}Te	2.38	2.09757E-33	2.29356E-13	12.48	11.6		
^{116}Xe		^{112}Te	2.24	2.55514E-35	3.92084E-15	14.24		12.99	
			1.85	5.29179E-41	4.49772E-21	20.19	19.0		

Table 3. Logarithm of predicted half-life time and other characteristics of ^{24}Mg emission from various Xe isotopes. Q values are taken from [5,6,22].

Parent nuclei	Daughter nuclei	Q value (MeV)	Penetrability P	Assault frequency	Decay constant	$\log_{10}(T_{1/2})$		
						Present	PCM	ASAFM
^{108}Xe	^{84}Mo	26.58	2.12428E-75	7.20012E+20	1.52951E-54	53.66	50.67	
^{110}Xe	^{86}Mo	28.88	4.61785E-67	7.82315E+20	3.61261E-46	45.28	41.25	
^{112}Xe	^{88}Mo	29.43	7.78753E-65	7.97214E+20	6.20833E-44	43.05	38.69	
^{114}Xe	^{90}Mo	27.77	7.45049E-70	7.52247E+20	5.60461E-49	48.09	44.59	
		27.19	7.23676E-72	7.36535E+20	5.33013E-51	50.11		48.1
^{115}Xe	^{91}Mo	27.46	1.00219E-70	7.43849E+20	7.45478E-50	48.97		47.1
^{116}Xe	^{92}Mo	28.13	3.05184E-68	7.61999E+20	2.32550E-47	46.47	42.80	
		27.72	1.22867E-69	7.50892E+20	9.22599E-49	47.88		46.3

and ^{28}Si emissions from various Xe isotopes. It is found that our predicted half-life time values lie close to those values reported by Kumar and collaborators [6] based on PCM and those values of Poenaru *et al* [5,22] based on ASAFM. Also ^{4}He, ^{8}Be, ^{12}C and ^{16}O emissions are found to be well within the present upper limit for measurements ($T_{1/2} < 10^{30}$ s). It is found that ^{8}Be emission from ^{108}Xe ($T_{1/2} = 6.17 \times 10^{8}$ s) and from ^{110}Xe ($T_{1/2} = 5.39 \times 10^{8}$ s) is the most favourable for measurements. These results are awaiting experimental confirmation. Lowest half-life time value for ^{8}Be emission from ^{108}Xe stress the role of doubly magic ^{100}Sn in cluster decay process which agree with our earlier observation [10,12]. In the case of ^{8}Be from ^{110}Xe the daughter is $^{102}_{50}\mathrm{Sn}_{52}$ which lies close to the doubly magic $N = Z = 50$ shell. Most probable α-emitter is ^{108}Xe (for $Q = 6.49$ MeV, $\log_{10}(T_{1/2}) = -10.2$ s) since its daughter $^{104}_{52}\mathrm{Te}_{52}$ also lies close to the doubly magic $N = Z = 50$ shells. In cluster radioactivity it is experimentally established that the daughter nuclei are doubly magic or near doubly magic. Experimental data available are α-decay half-life time and our calculated logarithm of half-life time value for ^{4}He emission from ^{110}Xe is -0.39 s which agrees with the experimental value [23] which is -0.4 s.

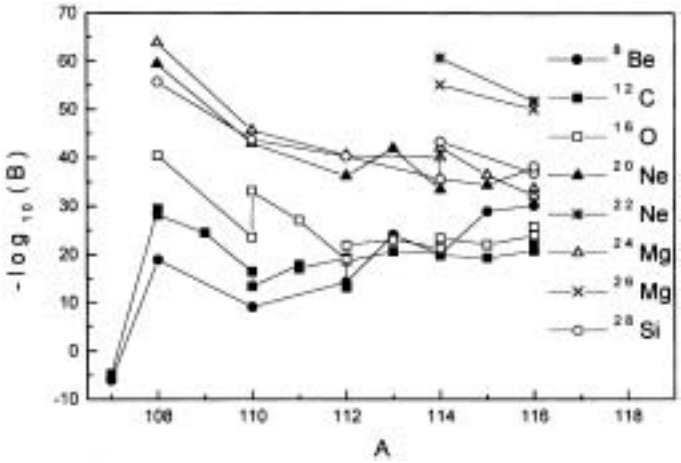

Figure 2. Negative logarithm of branching ratio vs. mass of Xe parents for various cluster emissions.

The branching ratio B of cluster decay with respect to α-emission is given by

$$B = \frac{\lambda_{\text{cluster}}}{\lambda_{\text{alpha}}} = \frac{T_{1/2}^{\text{alpha}}}{T_{1/2}^{\text{cluster}}}. \tag{13}$$

Figure 2 represents negative logarithm of the branching ratio, $-\log_{10}(B)$ vs. A for various clusters from different Xe isotopes. The experimental half-life time for respective α-decay $T_{1/2}^{\text{alpha}}$ are taken from Royer [23]. Using presently available technique the longest measured life-time is of the order of 10^{30} s and lowest measurable branching ratio is almost 10^{-19}. Branching ratio calculations predict that ^{8}Be emissions from ^{108}Xe and ^{110}Xe are the most favourable for measurements.

In the present model, cluster formation probability is taken as unity for all clusters irrespective of their masses. So the present model differs from PCM by a factor P_0, the cluster formation probability. The proximity formula used by the present model (eqs (4), (5)) and PCM (eqs (10), (11)) are the same except for the matching point ε-value which is 1.9475 in the present model and 1.2511 in PCM. But we took the contribution of internal part (overlap region) of the barrier in penetrability calculation. This is the reason for identical values for $\log_{10}(T_{1/2})$ for the present model and PCM. (For e.g. in the case of ^{28}Si emission from ^{116}Xe, Present = 51.07, PCM = 50.90 and for ^{22}Ne emission from ^{116}Xe, Present = 66.00, PCM = 66.35). The centrifugal term $V_\ell = \hbar^2\ell(\ell+1)/2\mu r^2$ is not considered for our calculation since ℓ values involved are small ($\approx 5\hbar$) and its contribution to half-life time are shown to be small [15].

Figure 3 represents Geiger–Nuttall plots for $\log_{10}(T_{1/2})$ vs. $Q^{-1/2}$ for ^{4}He, ^{8}Be, ^{12}C, ^{16}O, ^{20}Ne, ^{24}Mg and ^{28}Si emissions from various Xe isotopes. These plots are found to be linear with different slopes and intercepts. The equations for these plots are

$$\log_{10}(T_{1/2}) = XQ^{-1/2} + Y. \tag{14}$$

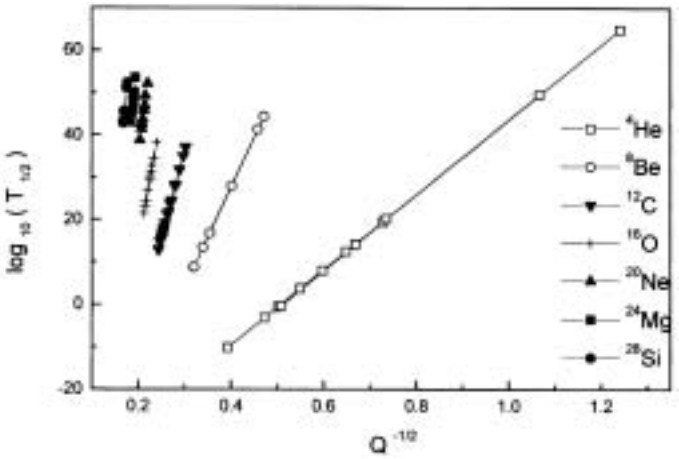

Figure 3. Geiger–Nuttall plot for $\log_{10}(T_{1/2})$ vs. $Q^{-1/2}$ for various clusters from different Xe isotopes.

The slope X and intercept Y values for various clusters are given in table 4. Geiger–Nuttall plots for $\log_{10}(T_{1/2})$ vs. $-\ln P$ for ^{4}He, ^{8}Be, ^{12}C, ^{16}O, ^{20}Ne, ^{24}Mg and ^{28}Si emissions from various Xe isotopes are also found to be linear. Figure 4 represents Geiger–Nuttall plots for $\log_{10}(T_{1/2})$ vs. $-\ln P$ for ^{4}He, ^{8}Be and ^{12}C emissions from various Xe isotopes. We would like to point out that Geiger–Nuttall law is for pure Coulomb potential but from our present study it is found that inclusion of proximity potential will not produce much deviation to the linear nature of these Geiger–Nuttall plots which agrees with our earlier observations [10–12]. We would like to mention that the presence of proximity potential (nuclear structure effect) and shell effect (through Q value) are evident from the observed variation in slope and intercept of Geiger–Nuttall plots for different clusters from Xe parents.

For ^{4}He emission from ^{108}Xe we used two Q values, 0.88 MeV taken from Poenaru *et al* [5] and 6.49 MeV taken from Satish Kumar *et al* [6]. It is found that the calculated $\log_{10}(T_{1/2})$ values for both Q values for the same parent lie on the straight

Table 4. Slope and intercept values of Geiger–Nuttall plots for different clusters from various Xe isotopes.

Emitted cluster	Slope X	Intercept Y
^{4}He	88.5811	−44.9384
^{8}Be	236.0719	−66.8178
^{12}C	407.5291	−85.9697
^{16}O	594.7938	−104.4178
^{20}Ne	792.8314	−122.3308
^{24}Mg	1066.3716	−153.7404
^{28}Si	1034.7248	−130.3360

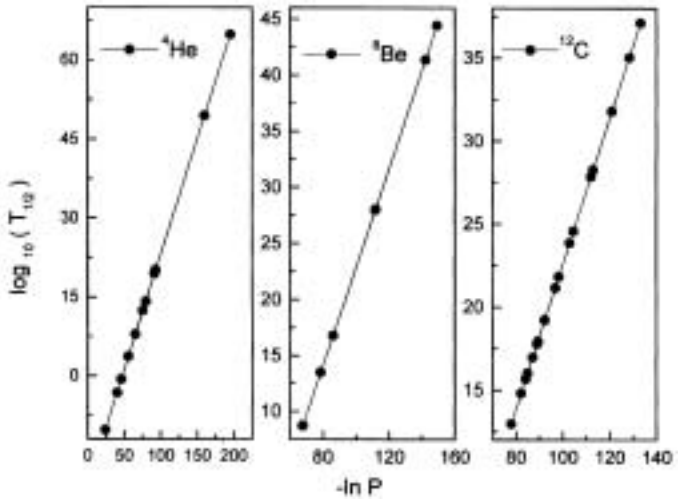

Figure 4. Geiger–Nuttall plot for $\log_{10}(T_{1/2})$ vs. $-\ln P$ for ^{4}He, ^{8}Be and ^{12}C emissions from various Xe isotopes.

line for two Geiger–Nuttall plots (Figures 3 and 4). This is due to the fact that assault frequency $\nu = 2E_\nu/h$, is related to Q value given by eq. (9). Increased Q value will increase ν which will reduce $T_{1/2}$ value. So both $\log_{10}(T_{1/2})$ values lie on the straight line for the two Geiger–Nuttall plots.

When the logarithm of half-life time for ^{8}Be emission from ^{108}Xe are compared with that from heavier isotopes up to ^{116}Xe, it is found that $\log_{10}(T_{1/2})$ increases from 8.732 s (for ^{108}Xe, $Q = 9.77$ MeV) to 44.45 s (for ^{116}Xe, $Q = 4.50$ MeV). All these cases refer to doubly or near doubly magic ^{100}Sn daughter. This points to the fact that neutron excess in the parent will slow down the cluster decay process. These findings are supporting our earlier observation in the case of Ba and Ce isotopes [10,12].

References

[1] A Sandulescu, D N Poenaru and W Greiner, *Fiz. Elem. Chastits At. Yadra* **11**, 1334 (1980); *Sov. J. Part. Nucl.* **11**, 528 (1980)
[2] R K Gupta, in *Heavy elements and related new phenomena* edited by R K Gupta and W Greiner (World Scientific Publication, Singapore, 1999) vol. 1, p. 536
[3] H J Rose and G A Jones, *Nature (London)* **307**, 245 (1984)
[4] R K Gupta, S Singh, R K Puri and W Scheid, *Phys. Rev.* **C47**, 561 (1993)
[5] D N Poenaru, D Schnabel, W Greiner, D Mazilu and R Gherghescu, *At. Data Nucl. Data Tables* **48**, 231 (1991)
[6] S Kumar, D Bir and R K Gupta, *Phys. Rev.* **C51**, 1762 (1995)
[7] G Shanmugam, G M Carmel Vigila Bai and B Kamalaharan, *Phys. Rev.* **C51**, 2616 (1995)
[8] Yu Ts Oganessian, Yu A Lazarev, V L Mikheev, Yu A Shirokovsy and S P Tretyakova, *Z. Phys.* **A349**, 341 (1994)

[9] A Guglielmetti, B Blank, R Bonetti, Z Janes, H Keller, R Kirchner, O Klepper, A Piechaczek, A Plochocki, G Poli, P B Price, E Roeckl, K Schmidt, J Szeryo and A J Westphal, *Nucl. Phys.* **A583**, 867c (1995)
[10] K P Santhosh and Antony Joseph, *Pramana – J. Phys.* **55**, 375 (2000)
[11] K P Santhosh and Antony Joseph, *Proceedings of the National Symposium on Radiation Physics* (Amritsar, India, 2001) p. 338
[12] K P Santhosh and Antony Joseph, *Pramana – J. Phys.* **58**, 611 (2002)
[13] J Blocki, J Randrup, W J Swiatecki and C F Tsang, *Ann. Phys. (N.Y.)* **105**, 427 (1977)
[14] J Blocki and W J Swiatecki, *Ann. Phys. (N.Y.)* **132**, 53 (1981)
[15] D N Poenaru, M Ivascu, A Sandulescu and W Greiner, *Phys. Rev.* **C32**, 572 (1985)
[16] Y J Shi and W J Swiatecki, *Nucl. Phys.* **A438**, 450 (1985)
[17] S S Malik and R K Gupta, *Phys. Rev.* **C39**, 1992 (1989)
[18] W D Myers and W J Swiatecki, *Nucl. Phys.* **81**, 1 (1966)
[19] G Shanmugam and B Kamalaharan, *Phys. Rev.* **C38**, 1377 (1988)
[20] D N Poenaru, D Mazilu and M Ivascu, *J. Phys.* **G5**, 1093 (1979)
[21] A J Sierk, *Phys. Rev. Lett.* **55**, 582 (1985)
[22] D N Poenaru, W Greiner, K Depta, M Ivascu, D Mazilu and A Sandulescu, *At. Data Nucl. Data Tables* **34**, 423 (1986)
[23] G Royer, *J. Phys.* **G26**, 1149 (2000)